Organic Conjugated Trimers with Donor–Acceptor–Donor Structures for Photocatalytic Hydrogen Generation Application

Xiaojiao Yuan, Cong Wang, Lorenzo Vallan, Anh Thy Bui, Gediminas Jonusauskas, Nathan D Mcclenaghan, Chloé Grazon, Sabrina Lacomme, Cyril Brochon, Hynd Remita, et al.

▶ **To cite this version:**

Xiaojiao Yuan, Cong Wang, Lorenzo Vallan, Anh Thy Bui, Gediminas Jonusauskas, et al.. Organic Conjugated Trimers with Donor–Acceptor–Donor Structures for Photocatalytic Hydrogen Generation Application. Advanced Functional Materials, 2023, pp.2211730. 10.1002/adfm.202211730 . hal-03951365

HAL Id: hal-03951365
https://hal.science/hal-03951365

Submitted on 23 Jan 2023

HAL is a multi-disciplinary open access archive for the deposit and dissemination of scientific research documents, whether they are published or not. The documents may come from teaching and research institutions in France or abroad, or from public or private research centers.

L'archive ouverte pluridisciplinaire **HAL**, est destinée au dépôt et à la diffusion de documents scientifiques de niveau recherche, publiés ou non, émanant des établissements d'enseignement et de recherche français ou étrangers, des laboratoires publics ou privés.

Organic Conjugated Trimers with Donor-Acceptor-Donor Structures for Photocatalytic Hydrogen Generation Application

Xiaojiao Yuan,[a] Cong Wang,[b] Lorenzo Vallan,[a]* Anh Thy Bui,*[c,d] Gediminas Jonusauskas,[d] Nathan D. McClenaghan,[c] Chloé Grazon,[c] Sabrina Lacomme,[e] Cyril Brochon,[a] Hynd Remita,*[b] Georges Hadziioannou,[a] Eric Cloutet*[a]

[a] Laboratoire de Chimie des Polymères Organiques (LCPO-UMR 5629), Université de Bordeaux, Bordeaux INP, CNRS, F-33607 Pessac, France.

[b] Institut de Chimie Physique, UMR 8000 CNRS Université Paris-Saclay, 91405 Orsay, France.

[c] Institut des Sciences Moléculaires UMR 5255 CNRS/Université de Bordeaux 351, Cours de la Libération 33405 Talence Cedex, France.

[d] Laboratoire Ondes et Matière d'Aquitaine UMR 5798, CNRS/Université de Bordeaux 351, Cours de la Libération 33405 Talence Cedex, France.

[e] Bordeaux Imaging Center-Imagerie Electronique, Université de Bordeaux, 33076 Bordeaux Cedex.

Abstract: Organic donor-acceptor-donor (D-A-D) polymers or small molecules are widely investigated in organic solar cells (OSC) due to their broad light absorption, narrow band gap, excellent charge mobility and exciton seperation at the interface. However, studies of conjugated small molecules with D-A-D molecule structures as photocatalytically active materials are still rare. In this work, we give an unprecedented demonstration that photocatalytic activity can in fact be affected by tuning the D and A. Especially, the EBE trimer, comprising 3,4-ethylenedioxythiophene (E) and benzothiadiazole (B) units, exhibits the best photophysical, chemical and photocatalytic properties compared to other D-A-D combinations of D and A. Detailed kinetic studies show that all these trimers in organic solution present relatively long-lived and highly emissive photogenerated singlet excitons ($\tau = 4 – 13$ ns; $\phi_{em} = 0.5 – 0.9$) as judged by photoluminescence and transient absorption measurements, while in specific cases formation of long-lived triplet states can be identified. Organic microparticles of the trimers are efficiently formed in aqueous solution by nanoprecipitation, and rapid photoinduced electron release/injection to the solvent is evidenced spectroscopically. The results indicate that organic small molecule structures with D-A-D structures pave a new pathway for photocatalytic solar-to-chemical energy conversion of novel small organic molecules.

Keywords: Conjugated trimers, D-A-D, organic semiconductor, photocatalysis, hydrogen generation

1. Introduction

π-Conjugated polymers (CPs)/small molecules composed of alternating electron donor (D) and acceptor (A) moieties have triggered massive interest for organic electronic applications such as organic photovoltaic (OPV)[1] and organic field-effect transistor (OFET)[2, 3] owing to their facile processing, relatively high absorption, stability and accessible redox potentials.[4-10] Introducing D and A group to the conjugated backbone of the molecule would be possible to significantly increase the photon response and intramolecular charge transfer upon excitation.[11-13] However, conjugated small organic molecules with D-A-D structures are rarely explored for their photocatalytic solar fuel production although they possess distinct advantages compared with conjugated polymers.[14-16] For example, well-defined chemical structures with tunable structures and known molecular weights allow controllable band gap and energy levels by molecular engineering and crystalline characteristics of small molecules help solid long-range order and charge carrier transport. In particular, easy purification and no batch-to-batch variations prompt their commercial scale production and good dispersion and solubility in organic solvents increase the surface area during photocatalytic reactions.[17-20]

Recent results have shown that different oligomers with D-D, A-A, D-A-D and A-A-A present appreciable photocatalytic H_2 production activity in a mixture of triethylamine, methanol and water solution. Here, the dibenzo[b,d]thiophene sulfone oligomer composed of three repetitive units showed comparable photocatalytic activity (HER = 6550 ± 150 μmol h^{-1} g^{-1}; λ>295 nm; 3 wt% Pd loading) with respect to the corresponding polymer, thus demonstrating that high molar masses are not required in order to display high activity, while backbone planarity, bridgehead atom and chain length have a greater impact on the photocatalytic property.[21] Also, conjugated thiophene-based D-A-D trimers have been successfully employed for the intermolecular C-H functionalization of electron rich heteroaromatics with malonate derivatives, exhibiting activities comparable to the $[Ru(bpy)_3]Cl_2$ benchmark and indicating that conjugated trimers with D-A-D molecule structures are promising photocatalysts for chemical reactions.[22] Other effort has been devoted to designing D-A structured molecular photocatalysts by controlling local structures of oligomers or polymers for significantly enhanced photocatalytic activity.[23-27] For instance, D-A linear oligomers showed an improvement of charge separation leading to enhanced photocatalytic H_2 production activity compared with the A-A counterpart.[27]

Nevertheless, systematic exploration of the effects of D-A-D conjugated structures by alternating sequence of D and A on their photophysical, chemical, and photocatalytic activities

remain unexplored. In this work, we report the effect of D-A-D conjugated trimers formed by different D and A units on their photophysical, electronic and photocatalytic properties (see **Figure**

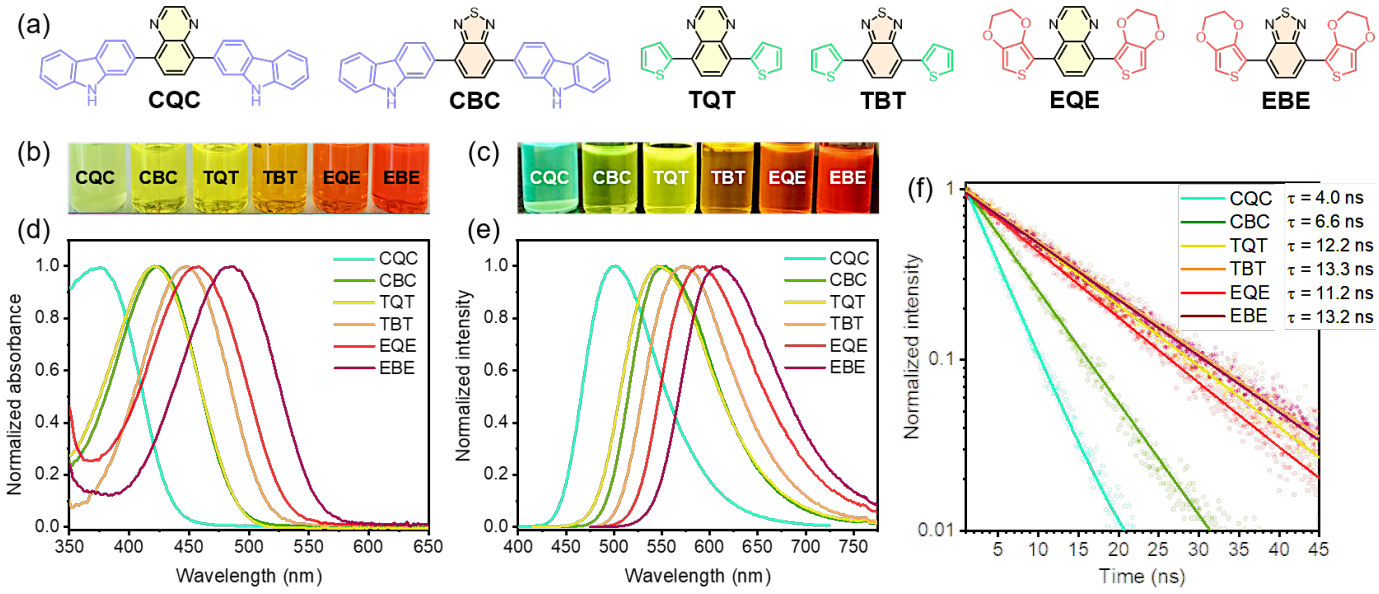

Figure 1. (**a**) Structural formulas of trimer photocatalysts. Photograph of catalysts in THF solution (**b**) under ambient light and (**c**) under UV light (λ = 365 nm). (**d**) Normalized UV-Vis absorption spectra of catalysts dissolved in THF. (**e**) Normalized steady-state photoluminescence spectra of trimers in THF. (f) Fluorescence decays obtained by time-resolved fluorescence spectroscopy with a streak camera (in photon counting mode), fitted by a monoexponential function.

1a and Figure S1). Benzothiadiazole (B) and quinoxaline (Q) are selected as acceptors due to their strong electron-withdrawing properties. Thiophene (T), 3,4-ethylenedioxythiophene (E), and carbazole (C) are most studied donor units in D-A polymers and oligomers owing to their strong electron-push ability. Besides, we provide a simple reprecipitation method to achieve stable suspensions of nanoaggregates, which makes the catalyst better dispersed in the aqueous solution. Lastly, the photocatalytic activity for H_2 generation with conjugated trimers under both ultraviolet and visible light irradiation is considered and detailed physico-chemical measurements are described below. To our knowledge, we are the first to systematically report the effects of conjugated trimers formed by different D and A units on their photophysical, chemical, electronic, and photocatalytic properties, which will pave the way for the diverse applications of D-A-D conjugated trimers including photocatalytic solar-to-chemical energy conversion.

2. Results and discussion

2.1 Catalysts characterizations

Conjugated trimers were synthesized by Pd (0)-catalyzed Suzuki-Miyaura cross-coupling or Stille cross-coupling reactions. The synthetic details and the ^{1}H HMR and ^{13}C NMR characterizations are described in the Electronic Supporting Information, ESI (**Scheme S1-6, Figure S2-S13**). Thiophene (T), 3,4-ethylenedioxythiophene (E), and carbazole (C) were selected as electron donors, which were combined with different electron acceptors (benzothiadiazole (B) and quinoxaline (Q)) to form D-A-D molecular structures (**Figure 1a**). With respect to typical conjugated polymer photocatalysts, these trimers have excellent solubility in organic solvents such as tetrahydrofuran (THF), dichloromethane, toluene, methanol and ethyl acetate.

The optical properties of the D-A-D conjugated trimers were studied in THF by absorption and steady-state fluorescence spectroscopy (see **Table 1**). **Figure 1b-c** shows the colour variation of trimers in THF solvent under ambient light and UV light (λ = 365 nm) irradiation. The broad, featureless bands in absorption spectra of the series of synthesized trimers dissolved in THF present strong absorption, from the near UV (λ_{max} = 376 nm, ε = 17,500 $M^{-1}cm^{-1}$ for CQC) with different variants spanning the visible spectral region (λ_{max} = 486 nm, ε = 11,800 $M^{-1}cm^{-1}$ for the most red-shifted EBE) (**Figure 1d**), and intense fluorescence emission with quantum yields comprised between 0.48 and 0.83 (**Table S1**). The type of donor unit in the D-A-D structure greatly affects both absorption and emission wavelengths, since a bathochromic shift is observed for the series C < T < E. Notably, the red-edge absorption of EBE extends to 575 nm, surpassing most organic semiconductor photocatalysts used for hydrogen production, in this regard.[28-30] Significant Stokes' shifts in emission are noted in each case (in the range 4000 - 6000 cm^{-1}), as often observed for dye molecules with push-pull character (see **Table S1**).

Room temperature emission maxima range from (λ_{max} = 501 nm for CQC to λ_{max} = 608 nm for EBE), with high quantum yield emission values (Φ_{em} = 0.48 – 0.83). Trimers flanked by thiophene moieties appear to be the most emissive, followed by those comprising carbazole and EDOT variants. Fluorescence lifetimes are relatively long for these small organic emitters, and are consistent with the observed quantum yields. As a result, intersystem crossing (ISC) to form long-lived dark states is anticipated to be inefficient. Indeed, transient absorption spectroscopy on the series revealed this to be the case with transient decays mirroring changes in fluorescence (see ESI), with one notable exception CQC. Here, formation of a long-lived state was observed, attributed to ISC giving rise to a triplet state in around 30% of excited molecules ($k_{ISC} = 2.7 \times 10^{8}$). Solid-state fluorescence emission spectra (**Figure S14**) show red-shifted emission compared with that in solution, indicating strong intermolecular interactions. Fluorescence excitation spectra are equally consistent with red-shifted absorption (vide infra).

The solid powder form of the trimers could not be efficiently dispersed in water directly. However, the insoluble solid trimers can be homogeneously dispersed in aqueous media by means of a simple reprecipitation method, achieving stable suspensions of nanoaggregates. Here, a THF solution of the trimer was rapidly injected into an excess volume of water and finally THF was removed under vacuum giving a stable and homogeneous particle dispersion. This strategy overcomes the low solubility in water intrinsic of these molecules and ensures a large active particle surface area, which is desirable for photocatalysis (**Figure 2a and Figure S15**). Dynamic light scattering (DLS) shows that the EBE particles have a broad size distribution due to particle aggregation in THF/H_2O solution (**Table S2 and Figure S16**). Meanwhile, TBT (421 ± 33 nm) and CBC (314 ± 9 nm) displayed a rather uniform size distribution. Interestingly, the absorption and emission spectra of EBE in THF/H_2O and THF/H_2O/TEOA suspension, where triethanolamine (TEOA) serves as a sacrificial hole scavenger in H_2 production experiments (see below), are strongly red shifted with respect to the spectra of EBE in THF. This is consistent with J-aggregation, which may help long-range order and charge carriers' transport inside the nanocrystals (**Figure 2 and Figure S17-19**). Note that it is unclear whether aggregation is generally beneficial for photocatalytic performance, although one study showed that aggregation enables high photocatalytic activity by intermolecular interactions.[31]

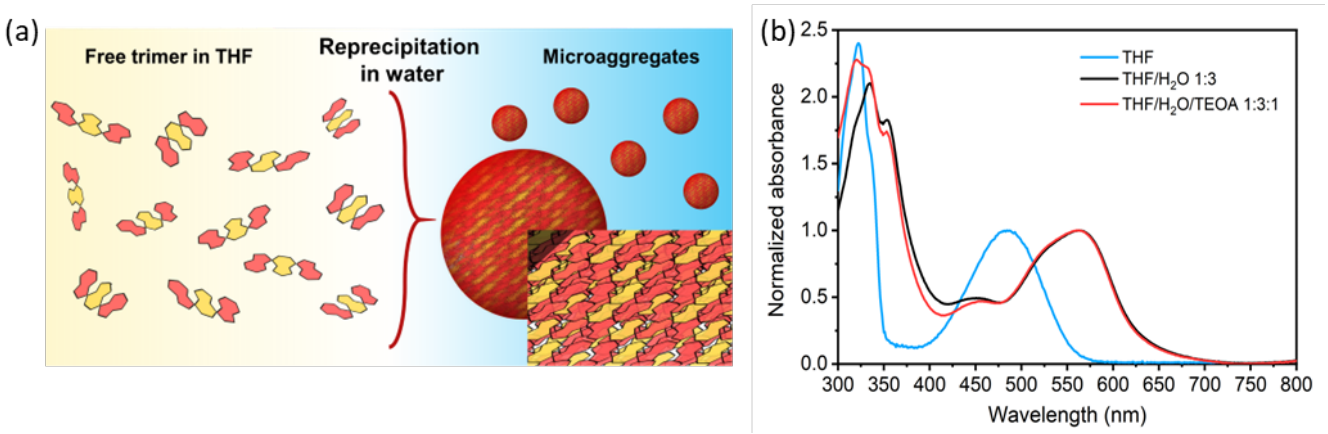

Figure 2. (**a**) The scheme of the reprecipitation method. (**b**) Normalized absorption spectra of EBE in THF (OD < 0.1), and of EBE in THF/H_2O 1:3 (volume ratio) and THF/H_2O/TEOA 1:3:1 (volume ratio), after a line subtraction treatment.

Considering EBE, SEM and AFM analyses show clear cubic crystals with different sizes (**Figure 3a-b, Figure S20-21**). The morphology of other trimers was shown in **Figure S20** and **Figure S21**. TEM (**Figure 3c-d**) and a Fourier transform (insert in Figure 3c) reveal the crystallinity of EBE. Typically, the crystalline properties of small molecules help solid long-range order and charge carrier transport. XRD (X-Ray Diffraction) further demonstrate that all these conjugated trimers have good crystallinity (**Figure S22**). EDS (energy dispersive spectroscopy) mapping shows the chemical composition of the trimers are S, C, and O, which indicates the purity of the samples (**Figure 3e-g**). No additional Pd particles were observed, confirming the low Pd residue. Thermogravimetric analysis (TGA) indicated that EBE and EQE are thermally stable in a nitrogen atmosphere up to 270 ˚C and other trimers present relatively poor thermal stability (**Figure S23**).

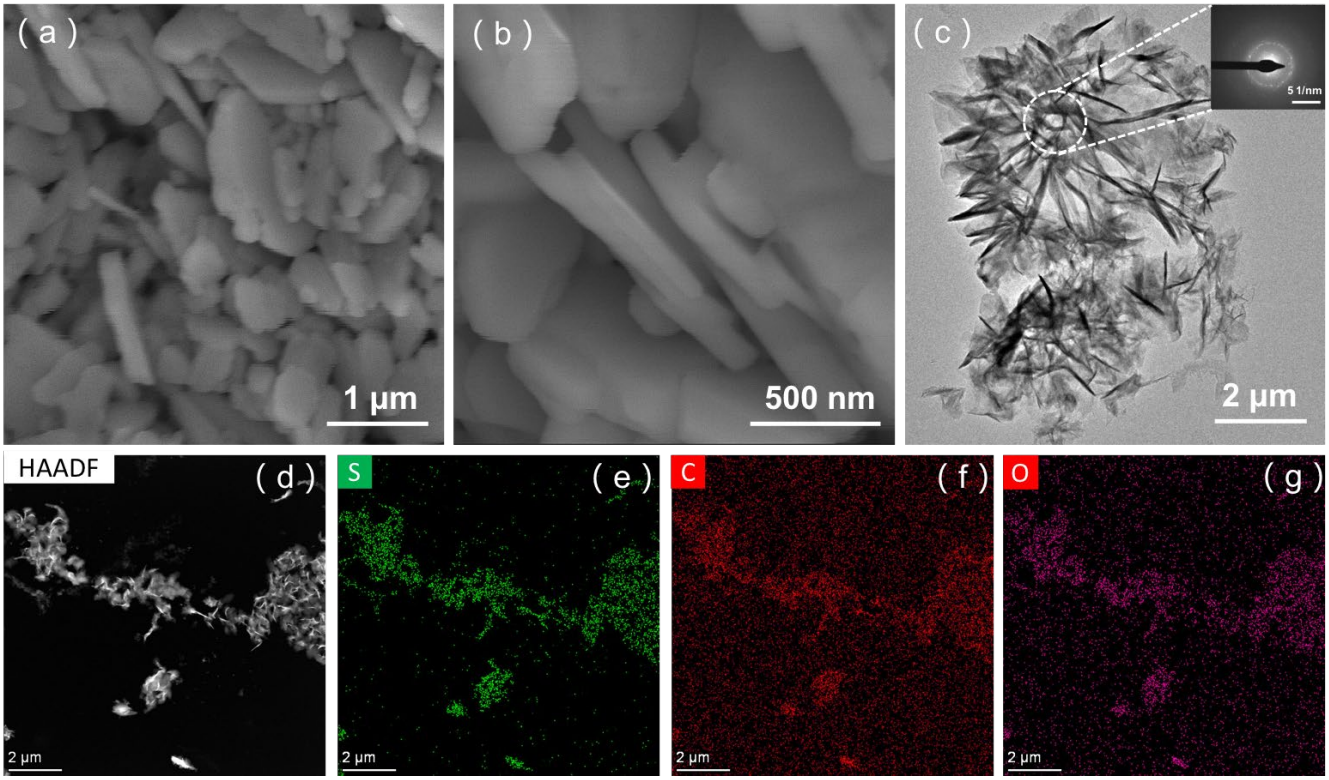

Figure 3. (**a-b**) SEM images, (**c**) TEM image and Fourier transform (insert image), (**d**) HAADF-STEM image, (**e**) S element of HAADF-STEM image, (**f-g**) the element mapping of EBE trimer.

Surface wettability is one of the key factors of heterogeneous photocatalysts to enhance their photocatalytic behaviour. For most polymer photocatalysts, their inherent apolar nature makes dispersion in aqueous solution more difficult, leading to low activity.[32] **Figure S24** shows the image of a water droplet placed on the trimer-film/glass. The trimers may be considered hydrophilic with around 40~60° contact angles, except that of TQT (106.6°). The hydrophilic property of trimers can

increase the contact between the trimer catalysts and the water, which may help to improve the photocatalytic performance of trimers. The optical absorption property of trimers in the solid state were investigated by UV-Vis diffuse reflectance spectroscopy (DRS), and all the trimers exhibit broad light absorption (**Figure 4a**). However, CQC, TQT and CBC show lower absorption in the visible region compared to EBE, EQE, TBT. Accordingly, the optical band gaps of trimers are determined on applying the Tauc equation (**Figure 4b**). The estimated band gap (E_g) of EBE, EQE, TBE, TQT, CBC and CQC are 1.94, 2.08, 2.04, 2.24, 2.36 and 2.63 eV, respectively (exciton binding energy of trimers was not considered), which are much smaller than the band gap of TiO_2 (3.2 eV). These narrow band gaps enhance the light-harvesting capability of the trimers and induce their absorption in the visible range. The LUMO (lowest unoccupied molecular orbital) levels are estimated by cyclic voltammetry (CV) and the HOMO levels are calculated by E_g - E(LUMO). Their band positions indicate that trimers are thermodynamically suited to drive reduction of protons to hydrogen since their reduction potentials are more negative than the potential of proton reduction ($2H^+ + 2e^- \rightarrow H_2$, E = -0.41 V *vs.* NHE at pH = 7) (**Figure 4c-d and Figure S25**). In addition, electrochemical impedance spectroscopy (EIS) allowed examination of the interface charge transfer resistances of the electrode materials. The smallest semicircles in the Nyquist plots for EBE and TBT (**Figure 4e**) indicate the faster and more efficient interfacial charge transfer ability of these two trimers with respect to the others, which is favorable with higher photocatalytic activity as shown below.

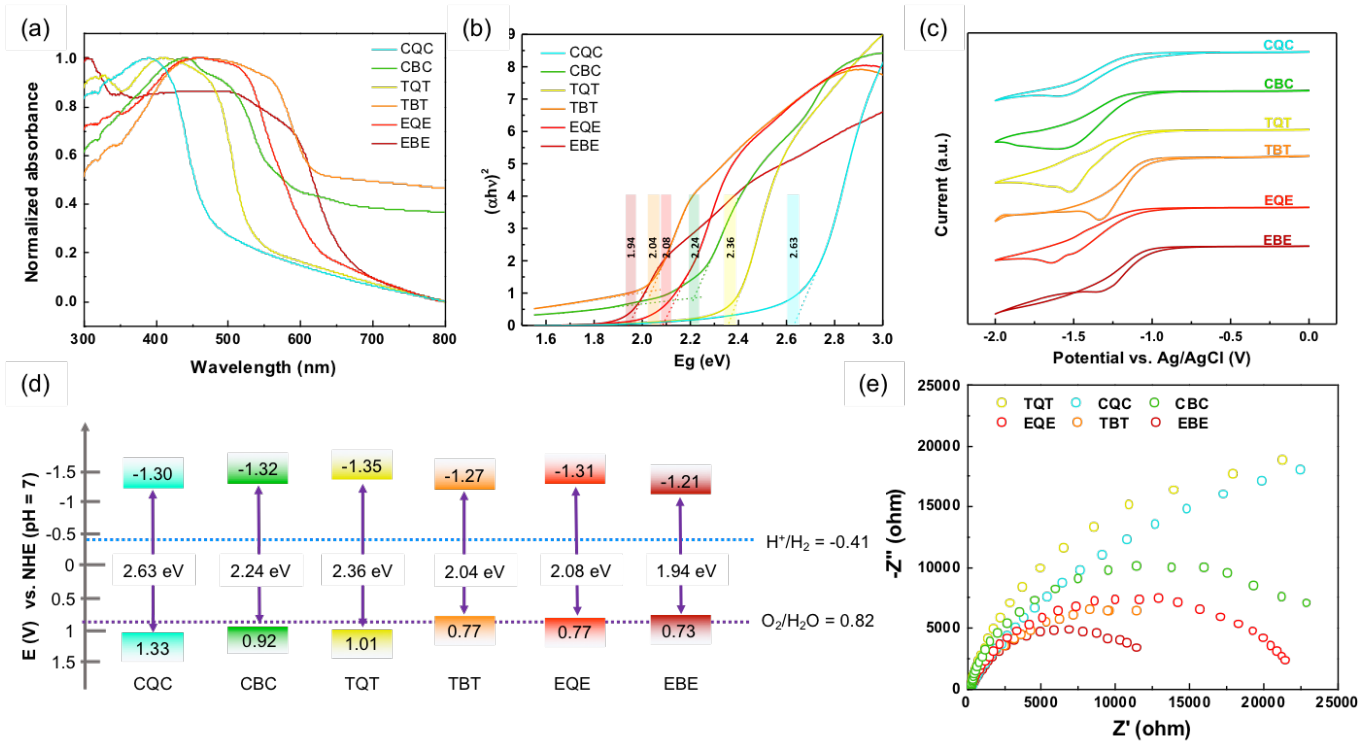

Figure 4. (**a**) DRS absorption spectra of the samples measured in the solid state (normalized intensities); (**b**) Calculated band gap from Tauc plots; (**c**) Cyclic voltammetry plots (reduction scans) of trimers in acetonitrile solution and 0.1 M tetrabutylammonium perchlorate; (**d**) Experimentally determined HOMO and LUMO energy levels of samples; (**f**) Nyquist plots of EIS for trimers/FTO electrodes under UV-Vis light irradiation.

2.2 Photocatalytic H_2 performance and kinetic study

Photocatalytic processes generally harness light absorption to generate charge carriers (electron-hole pairs), followed by charge separation and transportation, followed by redox reactions on the photocatalyst surface.[33] Upon excitation, the populated LUMO of the trimer can

Table 1. photophysical, electronic, and photocatalytic properties of trimers									
Samples	**λ_{abs} [a] (nm)**	**λ_{em} [b] (nm)**	**τ_{avg} [c] (ns)**	**HOMO [f] (eV)**	**LUMO [e] (eV)**	**E_g [b] (eV)**	**Residual Pd (wt %)**	**HER_{UV-Vis} [g] (μmol h^{-1} g^{-1})**	**HER_{Vis} [g] (μmol h^{-1} g^{-1})**
EBE	486	608	13.4	0.73	-1.21	1.94	0.04	277	142
EQE	458	591	11.7	0.77	-1.31	2.08	0.01	104	26
TBT	448	569	13.2	0.77	-1.27	2.04	0.00	231	46
TQT	422	548	12.3	1.01	-1.35	2.36	0.00	72	13
CBC	425	553	6.3	0.92	-1.32	2.24	0.30	86	15
CQC	376	501	4.0	1.33	-1.30	2.63	0.33	90	18

[a] UV-Vis absorption maximum wavelength; [b] Fluorescence emission upon excitation at their absorption maximum wavelength; [c] Average fluorescence lifetime; [d] HOMO values for the trimers can be estimated from the corresponding LUMO and E_g values; [e] Determined by cyclic voltammetry (CV) (vs Fc/Fc^+) in acetonitrile and 0.1 M tetrabutylammonium hexafluorophosphate (TBAHFP); [f] Optical band gap determined by Kubelka-Munk-transformed reflectance spectra; [g] HER: hydrogen evolution rate; conditions: 20 mL of 25% vol TEOA/H_2O and irradiated by a 300 W Xe lamp (UV-Vis) or $\lambda \geq 420$ nm (Vis).

thermodynamically drive proton reduction, while the sacrificial donor (TEOA) is oxidized via the HOMO of the trimer because it requires less thermodynamic potential than water oxidation ($2H_2O \rightarrow O_2 + 4\ H^+ + 4e^-$, E = 0.82 V *vs.* NHE at pH = 7), **Figure S25**. Photocatalytic H_2 evolution using trimers was first investigated under both ultraviolet and visible light irradiation ($\lambda \geq 420$ nm) in a TEOA/H_2O (1: 3, v/v) mixture. Meanwhile, H_2 was not detected in the dark or without trimer photocatalysts. Indeed, as illustrated in **Figure 5a-c and Figure S26**, all trimers are active for photocatalytic H_2 generation under both ultraviolet and visible light irradiation without any additional cocatalyst modification, and the hydrogen evolution rates of trimers proved higher than that of typical inorganic semiconductor TiO_2 under the same conditions. EBE exhibits the highest photocatalytic activity (HER = 275 μmol $h^{-1}g^{-1}$ under UV light and 142 μmol $h^{-1}g^{-1}$ upon visible irradiation), and apparent quantum yield (AQY) exceeding 2% at 400 to 450 nm, 1% at 550 nm and 0.3% at 600 nm, respectively, which is attributed to better wettability, broader light absorption, smaller band gap and longer lifetime of excitons (**Figure S27**). The activity of EBE slightly decreased after modification with 0.1 wt% Pt, which indicates Pt metal in the EBE may not assist in catalysing proton reduction (**Figure 5d**). The possible reasons are the reduction of multivalent Pt to Pt metal consuming part of the photogenerated electrons, and the excessive loading of Pt leads to the formation of the recombination center of photogenerated charger carriers and may block the active sites of conjugated trimers. In addition, the size, dispersion of Pt and the nature of support may also cause the reduction of the photocatalytic activity of Pt-EBE.[34, 35] The contents of residual Pd in trimers were measured by inductively coupled plasma-mass spectrometry (ICP-MS) (**Table 1**). EBE was found to contain 0.04 wt% residual Pd, while no residual Pd was detected in TBT. Likewise, we note that CBC and CQC show lower activity compared to that of EBE and TBT, although it had more Pd content (0.30 and 0.33 wt%, respectively). These results suggest that residual Pd may affect the photocatalytic reaction. Note that not only the loading amount of Pd, but

also its particle size, distribution, etc. will affect the activity.[35-37, 38] For comparison, all data for these trimers are collected in **Table S3**. It is noteworthy that EBE presents activity even in pure water for hydrogen production without scavengers and exhibits high stability during photocatalysis without a significant decline after 5 cycles (**Figure 5d-e**). The slight decrease in hydrogen production may be attributed to consumption of TEOA or sample aggregation. TEM and FTIR analysis of the recycled EBE reveals no changes in the spectrum compared with the starting material, suggesting that the chemical structure is stable during the photocatalytic H_2 evolution reaction (**Figure S28-S29**).

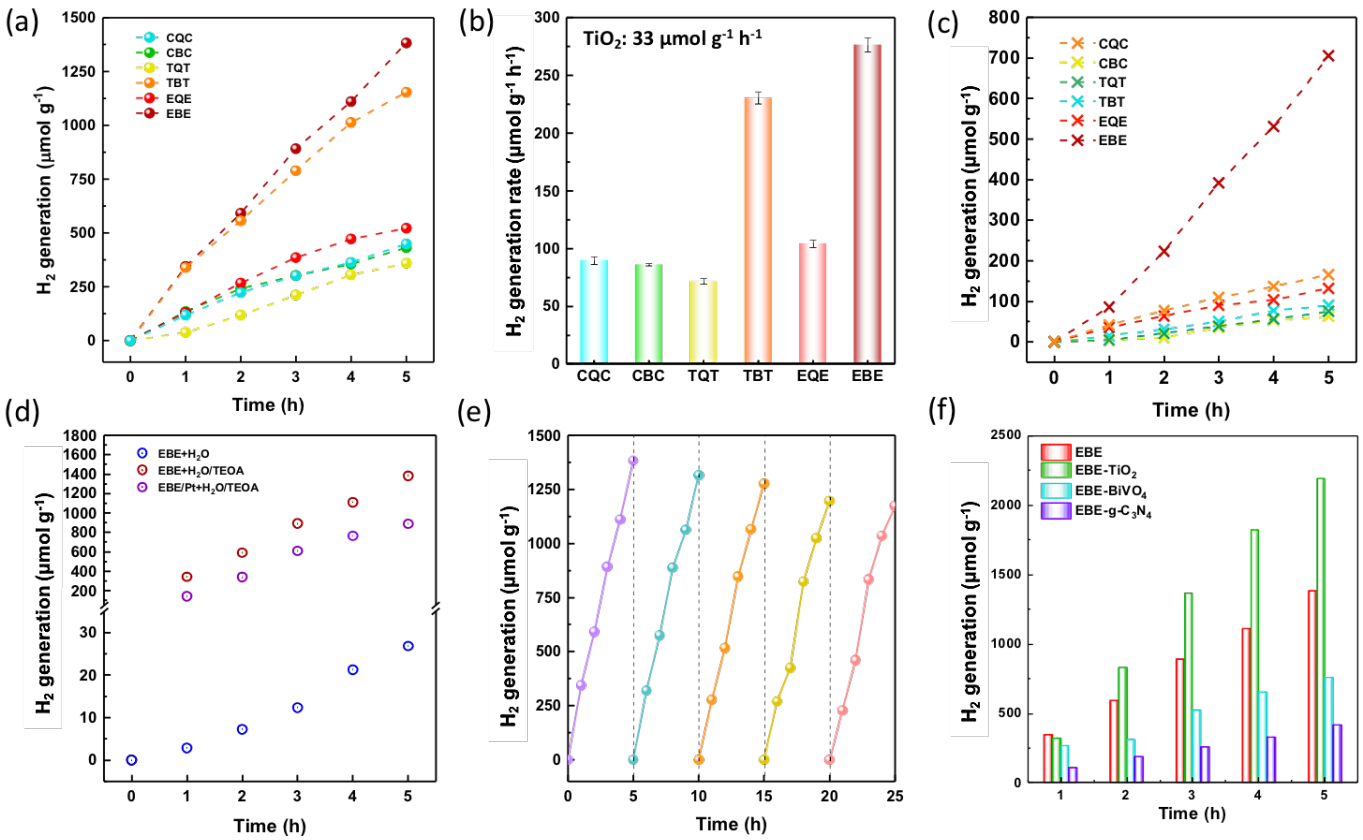

Figure 5. (**a**) Time course of photocatalytic H_2 generation for trimers under UV-Vis light; (**b**) Normalized H_2 production under UV-Vis light; (**c**) Time-course of photocatalytic H_2 generation for trimers under visible light ($\lambda \geq 420$ nm); (d) Photocatalytic H_2 generation for EBE trimer under different conditions (in pure water, water + TEOA, 0.1wt% Pt modification); (**e**) H_2 generation with cycling in the presence of EBE in TEOA/H_2O solution; (**f**). Time course of photocatalytic H_2 generation for EBE-based composites under UV-vis light.

Constructing hybrid materials containing the π conjugated structure provides unique advantages for photocatalysis, which can enhance the light absorption and stability of catalysts,[39] and the formed heterojunctions also exhibit more efficient charge separation and transfer through Schottky junctions.[40-42] We attempted to optimize the activity of EBE by introduction of benchmark semiconductors (such as TiO_2, $BiVO_4$ and C_3N_4 as model inorganic and organic semiconductors) (**Figure 5f**). A major increase in photocatalytic H_2 production was obtained when the EBE was combined with TiO_2. The enhanced activity of EBE-TiO_2 is attributed to formation of a p-n heterojunction, as a result of TiO_2 lower-lying conduction band (E_{CB} = -0.5 V *vs.* NHE at pH = 7) and valence band (VB) levels (E_{VB} = 2.7 V *vs.* NHE at pH = 7) with respect to EBE, which is beneficial to the charge carrier seperation.[43] Lower hydrogen production was observed when EBE was combined with $BiVO_4$ or C_3N_4. The absorption of EBE based composites is higher in the visible region compared with pure TiO_2, $BiVO_4$ or C_3N_4 (**Figure S30-32**). The dynamics of charge-carriers in EBE-TiO_2 composites at different wavelengths was investigated by time-resolved microwave conductivity (TRMC), **Figure S33-35**. A flat and higher signal intensity indicates less recombination and good charge carrier separation in the EBE-TiO_2 composite, which favours the photocatalytic activity. We foresee that conjugated trimers or trimer-based composites may provide ample scope for photocatalytic solar fuel production.

To understand the high activity of EBE, further optical measurements were undertaken on particles in aqueous solution. Time-resolved luminescence decays show a shortened emission, satisfactorily fit by a stretched exponential, with a relatively narrow distribution (τ = 0.71 ns) showing strong intermolecular interaction in the particle (**Figure S36-46**). Interestingly, transient absorption spectroscopy (**Figure 6**) shows, following pulsed laser excitation (λ_{ex} = 532 nm), rapid formation of a rather broad absorption band spanning the visible spectral region and significantly different to that of solubilized free EBE (**Figure S41-42**). This is attributed to generation of hot solvated electrons, and thus offers compelling evidence for photoejection of an electron from the EBE particle to the solution.[44, 45] Variations of relative ΔA in the 400-500 nm region reflect varying absorptivity of the different radical distributions in each case (**Figure 6b**). Similarly, fast photoejection of an electron was observed in the presence (τ = 11 ns) or absence (τ = 12 ns) of the TEOA sacrificial reductant (**Figure 6c**). Spectral evolution on longer timescales (**Figure S44**) ultimately leads to a visible spectrum comprising negative signals corresponding to ground state bleaching (upon comparison with **Figure 2**), showing the organic particles is in a metastable, non-native state, and the other positive signal is attributed to absorption of the formed radical EBE

particle. The presence of TEOA reductant appeared to slow down the kinetics of radical EBE particle-photoejected electron recombination (τ = 12 ns vs 17 ns), further supporting the possibility of light-driven electron photoejection from the EBE particle to bulk solvent, which may participate in H_2 production.

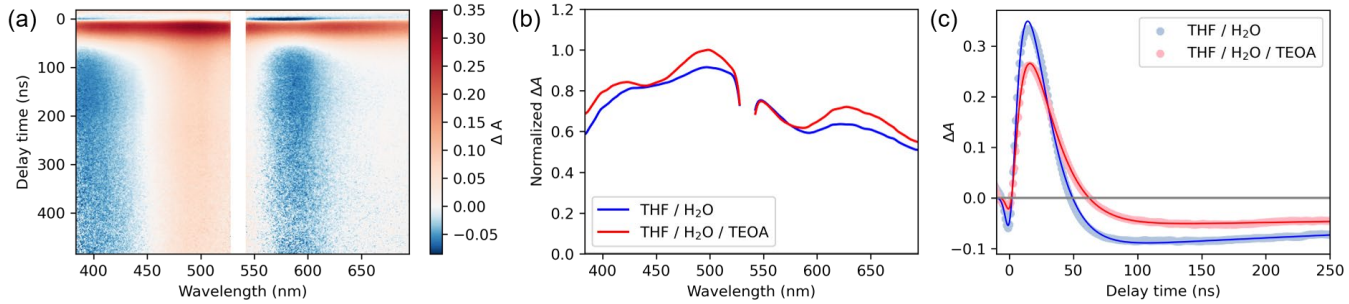

Figure 6. Transient absorption studies of EBE particles in aqueous media (λ_{ex} = 532 nm): (**a**) Transient absorption map in THF/H_2O/TEOA 1:3:1; (**b**) Transient absorption spectra at maximal ΔA (16 ns) in the absence (blue) or presence (red) of TEOA sacrificial reductant; (**c**) Kinetics of spectral change (spectral region 395–415 nm), showing generation of solvated hot photoelectrons followed by radical recombination (solid lines are data fits, according to model described in ESI).

3. Conclusions

A series of donor-acceptor-donor (D-A-D) conjugated trimers were systematically investigated for the effect of different D and A on their photophysical, chemical, electronic and photocatalytic hydrogen production properties. As expected, the choice of the donor and acceptor units makes it possible to tune the final optical properties of the material, with a clear impact on the photocatalytic performances. Stable suspensions in water/TEOA of trimer microaggregates were obtained by a simple reprecipitation method, overcoming trimers insolubility in water and ensuring large photocatalytic surface area. Particularly, EBE displays the highest H_2 generation activity among the series of trimers without additional cocatalyst modification (275 μmol h^{-1} g^{-1} and 142 μmol h^{-1} g^{-1} under UV and visible light irradiation, respectively). Appropriate energy band levels provide possibility of water splitting by rational design of molecular structures. Besides, the enhanced activity of EBE-TiO_2 demonstrates that organic-inorganic heterojunction construction is an efficient way for further improvement in the photocatalytic activity. This work opens new perspectives for small organic molecules, such as conjugated trimers, as promising photocatalysts for solar to chemical energy conversion.

Author Contributions

X. Yuan synthesized conjugated trimers, characterized and performed hydrogen generation experiments. L. Vallan co-supervised the synthesis, discussed the data and analysed the NMR results. C. Wang performed the electrochemical experiments. A. T. Bui, G. Jonusauskas and N. McClenaghan provided the transient absorption data. C. Grazon and A. T. Bui performed the measurement of fluorescence properties. S. Lacomme performed the TEM, STEM and EDS measurements. H. Remita supervised the photocatalytic experiments. C. Brochon, G. Hadziioannou and E. Cloutet co-supervised the project. The manuscript was written by X. Yuan. All authors have corrected and approved the final version of the manuscript.

Conflicts of interest

There are no conflicts to declare.

Acknowledgements

X. Yuan gratefully acknowledges the financial support for postdoctoral research by European Union's Horizon 2020 research and innovation program under the grant agreement No.800926 (HyPhOE). The authors thank Emile Decompte for DLS measurements. Catherine Denage (ICMCB-UMR5026) is acknowledged for the ICP-OES measurement.

Notes and references

1. Q. Shi, P. Cheng, Y. Li and X. Zhan, *Advanced Energy Materials*, 2012, **2**, 63-67.
2. M. Kim, S. U. Ryu, S. A. Park, K. Choi, T. Kim, D. Chung and T. Park, *Advanced Functional Materials*, 2020, **30**, 1904545.
3. H. Phan, M. Wang, G. C. Bazan and T. Q. Nguyen, *Advanced Materials*, 2015, **27**, 7004-7009.
4. H. Tang, C. Yan, J. Huang, Z. Kan, Z. Xiao, K. Sun, G. Li and S. Lu, *Matter*, 2020, **3**, 1403-1432.
5. H.-C. Wang, C.-H. Chen, R.-H. Li, Y.-C. Lin, C.-S. Tsao, B. Chang, S. Tan, Y. Yang and K.-H. Wei, *Solar RRL*, 2020, **4**, 2000253.
6. D. Hu, Q. Yang, H. Chen, F. Wobben, V. M. Le Corre, R. Singh, T. Liu, R. Ma, H. Tang and L. J. A. Koster, *Energy & Environmental Science*, 2020, **13**, 2134-2141.
7. L. Vallan, E. Istif, I. J. Gómez, N. Alegret and D. Mantione, *Polymers*, 2021, **13**, 1977.

8. D. Mantione, E. Istif, G. Dufil, L. Vallan, D. Parker, C. Brochon, E. Cloutet, G. Hadziioannou, M. Berggren and E. Stavrinidou, *ACS Applied Electronic Materials*, 2020, **2**, 4065-4071.
9. J. Li, X. Gao, L. Zhu, M. N. Ghazzal, J. Zhang, C.-H. Tung and L.-Z. Wu, *Energy & Environmental Science*, 2020, **13**, 1326-1346.
10. X. Yuan, D. Dragoe, P. Beaunier, D. B. Uribe, L. Ramos, M. G. Méndez-Medrano and H. Remita, *Journal of Materials Chemistry A*, 2020, **8**, 268-277.
11. P. Roy, A. Jha, V. B. Yasarapudi, T. Ram, B. Puttaraju, S. Patil and J. Dasgupta, *Nature communications*, 2017, **8**, 1-10.
12. L. O. Pålsson, C. Wang, A. S. Batsanov, S. M. King, A. Beeby, A. P. Monkman and M. R. Bryce, *Chemistry–A European Journal*, 2010, **16**, 1470-1479.
13. R. Tautz, E. Da Como, C. Wiebeler, G. Soavi, I. Dumsch, N. Fröhlich, G. Grancini, S. Allard, U. Scherf and G. Cerullo, *Journal of the American Chemical Society*, 2013, **135**, 4282-4290.
14. S. J. Moniz, S. A. Shevlin, D. J. Martin, Z.-X. Guo and J. Tang, *Energy & Environmental Science*, 2015, **8**, 731-759.
15. A. Kudo and Y. Miseki, *Chemical Society Reviews*, 2009, **38**, 253-278.
16. Y. Wang, A. Vogel, M. Sachs, R. S. Sprick, L. Wilbraham, S. J. Moniz, R. Godin, M. A. Zwijnenburg, J. R. Durrant and A. I. Cooper, *Nature Energy*, 2019, 1-15.
17. F. Zhang, D. Wu, Y. Xu and X. Feng, *Journal of Materials Chemistry*, 2011, **21**, 17590-17600.
18. Y. Lin and X. Zhan, *Accounts of chemical research*, 2016, **49**, 175-183.
19. B. Kan, M. Li, Q. Zhang, F. Liu, X. Wan, Y. Wang, W. Ni, G. Long, X. Yang and H. Feng, *Journal of the American Chemical Society*, 2015, **137**, 3886-3893.
20. S. D. Collins, N. A. Ran, M. C. Heiber and T. Q. Nguyen, *Advanced Energy Materials*, 2017, **7**, 1602242.
21. C. M. Aitchison, M. Sachs, M. A. Little, L. Wilbraham, N. J. Brownbill, C. M. Kane, F. Blanc, M. A. Zwijnenburg, J. R. Durrant and R. S. Sprick, *Chemical Science*, 2020, **11**, 8744-8756.
22. L. Wang, W. Huang, R. Li, D. Gehrig, P. W. Blom, K. Landfester and K. A. Zhang, *Angewandte Chemie International Edition*, 2016, **55**, 9783-9787.
23. H. Ou, X. Chen, L. Lin, Y. Fang and X. Wang, *Angewandte Chemie International Edition*, 2018, **57**, 8729-8733.
24. Z. A. Lan, G. Zhang, X. Chen, Y. Zhang, K. A. Zhang and X. Wang, *Angewandte Chemie International Edition*, 2019, **58**, 10236-10240.
25. Z.-A. Lan, W. Ren, X. Chen, Y. Zhang and X. Wang, *Applied Catalysis B: Environmental*, 2019, **245**, 596-603.

26. H. Yang, X. Li, R. S. Sprick and A. I. Cooper, *Chemical Communications*, 2020, **56**, 6790-6793.
27. Q. Wei, X. Yao, Q. Zhang, P. Yan, C. Ru, C. Li, C. Tao, W. Wang, D. Han and D. Han, *Small*, 2021, **17**, 2100132.
28. X. Wang, K. Maeda, A. Thomas, K. Takanabe, G. Xin, J. M. Carlsson, K. Domen and M. Antonietti, *Nature materials*, 2009, **8**, 76-80.
29. C. Hu, F. Chen, Y. Wang, N. Tian, T. Ma, Y. Zhang and H. Huang, *Advanced Materials*, 2021, **33**, 2101751.
30. C. B. Meier, R. Clowes, E. Berardo, K. E. Jelfs, M. A. Zwijnenburg, R. S. Sprick and A. I. Cooper, *Chemistry of Materials*, 2019, **31**, 8830-8838.
31. X. Yang, Z. Hu, Q. Yin, C. Shu, X. F. Jiang, J. Zhang, X. Wang, J. X. Jiang, F. Huang and Y. Cao, *Advanced Functional Materials*, 2019, **29**, 1808156.
32. Y. Bai, L. Wilbraham, H. Gao, R. Clowes, H. Yang, M. A. Zwijnenburg, A. I. Cooper and R. S. Sprick, *Journal of Materials Chemistry A*, 2021.
33. J. Kosco, F. Moruzzi, B. Willner and I. McCulloch, *Advanced Energy Materials*, 2020, **10**, 2001935.
34. J. Murcia, J. Navío and M. Hidalgo, *Applied Catalysis B: Environmental*, 2012, **126**, 76-85.
35. J. Kosco and I. McCulloch, *ACS Energy Letters*, 2018, **3**, 2846-2850.
36. J. Kosco, M. Sachs, R. Godin, M. Kirkus, L. Francas, M. Bidwell, M. Qureshi, D. Anjum, J. R. Durrant and I. McCulloch, *Advanced Energy Materials*, 2018, **8**, 1802181.
37. A. W. Prentice and M. A. Zwijnenburg, *Sustainable Energy & Fuels*, 2022, **6**, 3756-3767.
38. M. Avanthay, R. B. Bedford, C. S. Begg, D. Böse, J. Clayden, S. A. Davis, J.-C. Eloi, G. P. Goryunov, I. V. Hartung and J. Heeley, *Nature Catalysis*, 2021, **4**, 994-998.
39. T. Lv, Z. Jin, L. Zhang and Y.-J. Zeng, in *Optoelectronic Organic–Inorganic Semiconductor Heterojunctions*, CRC Press, 2021, pp. 315-350.
40. S. Singh, H. Chen, S. Shahrokhi, L. P. Wang, C.-H. Lin, L. Hu, X. Guan, A. Tricoli, Z. J. Xu and T. Wu, *ACS Energy Letters*, 2020, **5**, 1487-1497.
41. E. Shirman, T. Shirman, A. V. Shneidman, A. Grinthal, K. R. Phillips, H. Whelan, E. Bulger, M. Abramovitch, J. Patil and R. Nevarez, *Advanced Functional Materials*, 2018, **28**, 1704559.
42. X. Yuan, C. Wang, D. Dragoe, P. Beaunier, C. Colbeau-Justin and H. Remita, *Applied Catalysis B: Environmental*, 2021, **281**, 119457.
43. S. B. Rawal, S. Bera, D. Lee, D.-J. Jang and W. I. Lee, *Catalysis Science & Technology*, 2013, **3**, 1822-1830.
44. W. Marbach, A. Asaad and P. Krebs, *The Journal of Physical Chemistry A*, 1999, **103**, 28-32.

45. M. J. Bedard-Hearn, R. E. Larsen and B. J. Schwartz, *The Journal of chemical physics*, 2005, **122**, 134506.